Renewable Energy 132 (2019) 667–682

Contents lists available at ScienceDirect

Renewable Energy

journal homepage: www.elsevier.com/locate/renene

Preparation and performance investigation of a lignin-based solid acid catalyst manufactured from olive cake for biodiesel production

Arwa Sandouqa [a, *], Zayed Al-Hamamre [a, **], Jamil Asfar [b]

[a] Chemical Engineering Department, Amman, 11942, Jordan
[b] Mechanical Engineering Department, School of Engineering, The University of Jordan, Amman, 11942, Jordan

ARTICLE INFO

Article history:
Received 31 October 2017
Received in revised form
3 August 2018
Accepted 7 August 2018
Available online 10 August 2018

Keywords:
Lignin-based catalyst
Olive cake
Biodiesel
Solid acid catalyst

ABSTRACT

In this study, the olive cake was successfully developed and applied as a substrate to produce a lignin-based catalyst for biodiesel production. Three lignin-based solid acid catalysts were prepared from the incomplete carbonized alkali lignin using concentrated sulfuric acid. The catalyst underwent a detailed characterization analysis in terms of its functional groups of active sites, surface area, acid sites density and morphological structure. For the catalytic activity test, prepared catalysts were studied for their ability to catalyze both esterification and transesterification reactions of waste vegetable oil (WVO) ≈2 FFA (% w/w).

The results revealed that a sulfonated lignin-derived acid catalyst has a high potential to esterify waste vegetable oil to about (92%) conversion. Furthermore, it demonstrated about 57% conversion to fatty acid methyl esters (FAME) under the following optimum condition: sulfonation time of 1 h, catalyst loading of 10 wt %, the methanol-to-WVO molar ratio of 35:1, a reaction temperature of 65 °C and reaction time of 6 h. Also, the results showed that the lignin-based acid catalyst can be reused at least ten times with high FFA conversion (>75%).

1. Introduction

Globally, lignocellulosic feedstocks, including agro-waste, are abundantly produced and being a potential hazard to the environment and, consequently, to society. By contrast, these wastes are rich sources of cellulose, hemicellulose, and lignin. Therefore, these resources can go from being a hazardous risk to becoming generators of profit if they are turned into valuable products for other processes. Thus, reducing both price and demand for the main products [1]. Agriculture plays an important role in the economies of most of the countries in the Middle East. The contribution of the agricultural sector in Jordan's GDP is about 4.3% in 2017. The sector contribution of JOD 138 million in the January of 2018, showing a growth of 3.8% in comparison with the same period of 2017 [2]. Agricultural wastes are biomass residues that can be divided into two categories, namely the crop residues and the agro-industrial residues. Agro-industrial residues cover the whole range of biomass produced or discarded as by-products from processing crops. Crop residues include all plant residues that remain on the field after the collection and harvesting of crops, such as pulps, straws, stems, stalks, leaves, husks, shells, peels, bagasse, stubble, roots, etc [3].

Olive is an important cash crop that constitutes a prominent position in Jordan economy. The olive area in Jordan covers 77% of the tree-planted area and accounts for approximately 24% of the total cultivated area [4]. The produced olive cake processes as pressed blocks in the olive mills. Unfortunately, the olive cake is vastly underutilized. It is either used as domestic fuel in rural areas or left to be decomposed on open land, causing severe environmental problems, air pollution and affect the quality of groundwater. Each pressed ton of olive cake generates about a quarter of its quantity as waste and 1.5 m^3 of water which contains toxic phenol, high biological oxygen demand (BOD), and high chemical oxygen demand (COD). The total amount of olive cake reached about 37,000 tonnes in 2015 [5,6]. The major constituents of olive cake biomass are extractives, cellulose, hemicelluloses, and lignin [7]. Furthermore, the olive cake has a high calorific value (20.8 MJ/kg) and the ash content does not exceed 3.27 (w/w) %. These factors make olive cake biomass an excellent waste-to-energy resource in

* Corresponding author.
** Corresponding author.
E-mail addresses: a.sandouqa@ju.edu.jo (A. Sandouqa), z.hamamre@ju.edu.jo (Z. Al-Hamamre).

https://doi.org/10.1016/j.renene.2018.08.029
0960-1481/

Jordan. It can be used in a wide range of biochemical technologies and thermal processes, including but not limited to, combustion, gasification, and pyrolysis [6].

Biodiesel is a clean burning alternative fuel produced from renewable resources. The most common way to produce biodiesel is transesterification by the reaction of oil or fat with a low molecular weight alcohol, such as ethanol and methanol. Direct esterification can be carried out in the presence of a homogeneous or heterogeneous catalyst. The homogenous base catalyst is not recommended due to saponification and catalyst separation problems [8]. Two steps acid catalyzed pre-esterification by H_2SO_4 followed by alkali-catalyzed transesterification, has several drawbacks, these include equipment corrosion, difficulty in separation due to emulsion formation, reusability of catalyst and high energy and water consumption during purification. The best esterification catalyst might be still sulfuric acid. However, many studies have investigated, recently, the performance of heterogonous solid catalysts such as Zirconia, zeolite, sulfated tin oxide, etc. Over 90% conversion of both esterification and transesterification were reported. These catalysts improved the process efficiency, allowed continuous operation, environmentally friendly, has less corrosive effects, can be easily separated, recycled and regenerated and can reduce the biodiesel production cost [9,10].

The conversion of lignocellulosic material to valuable products (heterogeneous solid catalyst) requires an efficient fractionation method of the major components: hemicellulose (10–25%), cellulose (40–50%), and lignin (25–40%) [11]. Several processes have been suggested to convert various types of lignocellulosic biomass into lignin. In these processes, carbohydrates (cellulose and hemicelluloses) are hydrolyzed to their monomers, whereas the lignin isolation could be utilized as a source for phenolic polymers (phenyl propane units). The structure of such polymers depends on the plant source, plant age, part of the plant and the extractive method. Lignin contains several functional groups, phenolic hydroxyl, benzylic hydroxyl, and carbonyl groups which gives the importance and high potential of using it as a renewable source of biofuel and chemicals [12,13].

Bio-based heterogeneous catalysts (lignin-derived) that are manufactured by sulfonation of lignin are nontoxic, noncorrosive and can be easily recycled and activated. In particular, lignin-derived catalysts are able to catalyze both transesterification and esterification reactions at the same time in high economic and environmental way [14].

In the present work, the olive cake was used as a substrate for the production of lignin-based catalyst. The effect of activation and sulfonation time on the chemical and physical properties of lignin-based solid acid catalysts and its application to esterify WVO without pretreatment were studied. The catalysts experienced a detailed characterization analysis in terms of their functional groups of active sites, surface area, acid sites density and morphological structure. Further, the optimum variables for the esterification-transesterification reactions were determined.

2. Methodology

2.1. Materials

The olive cake was obtained from modern Jordanian olive mill (Husban Typical Squeezer, Madaba, Jordan, Latitude: 31°42′57″N, Longitude: 35°47′38″ E). For lignin extraction, sodium hydroxide (NaOH, 99%) was obtained from Gulf Coast Company (GCC). Sulfuric acid (H_2SO_4, 95–97%) was obtained from Merck Company. For catalyst preparation, Phosphoric acid (H_3PO_4) analytical grade (90%) was obtained from M&B Laboratory reagent Company. Sulfuric acid (H_2SO_4) analytical grade (98%) was obtained from Scharlau Company).

For the transesterification reaction waste vegetable oil (WVO), originally sunflower oil was obtained from the cafeteria of the school of engineering/The University of Jordan/Amman. The oil was spiked with the olive oil extracted from olive cake to increase its acid value to 3.67 mg KOH/g oil. Methanol of analytical grade (99.5%) was supplied also by Gulf Coast Company (GCC).

2.2. Procedure

2.2.1. Lignin extraction

Olive cake, in a solid-to-liquid ratio of 1:6, was placed in a reactor in aqueous 7.5% NaOH (w/w) solution. The reaction was kept under agitation for 90 min at a temperature of 90 °C. At the end of the reaction, the delignified material was recovered by filtration to obtain the black liquor without any fibrous materials. The black liquor (pH = 13.5) was treated by drop wise addition of concentrated H_2SO_4 (95–97%) until the pH was reached approximately 2. The lignin which became hydrophobic was precipitated. The precipitate was then isolated by filtration and washed several times with distilled water until neutralization (measured by pH meter). Finally, the recovered lignin was air dried, stored and considered as alkali lignin [15,16]. Lignin yield was calculated according to Eq. (1), where W_1 and W_2 are oven dry weight of the olive cake and produced alkali lignin respectively.

$$Yield(\%) = \frac{W_2}{W_1} \times 100\% \quad (1)$$

2.2.2. Catalyst preparation

The solid acid catalyst was produced from lignin by chemical activation, partial carbonization, and sulfonation according to the approach described by Pua et al. [17]. Olive cake alkali lignin powder (1–2 mm) was initially activated by impregnation in concentrated H_3PO_4 (90%) in a ceramic boat with (1:1) (solid to liquid) impregnation ratio at room temperature and for 1 h. After that, the activated lignin was dried at 105 °C and for 24 h to remove residual water. The carbonization of the dried impregnated lignin was performed in two-neck round bottom flask placed in a heating mantel (Electromantle, 500 ml, $T_{max} = 450$ °C) under N_2 flow. The carbonization temperature was set to 400 °C for 1 h activation time. The carbonized sample was cooled to room temperature under N_2 flow and then washed several times with hot and cold distilled water to remove residual chemicals [18]. The washed carbonized sample was dried at 105 °C and for 24 h. The bio-char yield was calculated based on the lignin weight and by using Eq. (2), where, M_1 and M_2 are the weight of produced char and lignin respectively [19].

$$Yield(\%) = \frac{M_1}{M_2} \times 100\% \quad (2)$$

Finally, the bio-char was sulfonated in a batch reactor set in an oil bath at (150 °C) by concentrated H_2SO_4 (98%) (1:10) (solid to liquid) ratio for different time (1, 5, 10 h). The catalyst was labeled as ($LACS_1$, $LACS_5$, and $LACS_{10}$).

Catalyst yield was calculated based on the lignin weight and by using Eq. (2), where, M_1 and M_2 are the weight of produced catalyst and char respectively.

The catalyst reusability was studied following the method described by Lokman et al. [20]. The used catalyst ($LACS_1$) was first washed with methanol and then with hexane to remove polar and non-polar compounds then dried to remove the residual solvents. The activity of the recycled catalyst was investigated at the

optimum biodiesel reaction parameters. Both esterification and transesterification conversion was tested.

2.2.3. Catalyst performance

The solid acid lignin-derived catalyst performance was investigated in one step biodiesel production from waste vegetable oil (WVO). Lignin-derived acid catalyst (>150 μm) were used. The reaction was carried out in a two-neck round bottom flask equipped with a condenser and thermometer. The flask reactor was immersed in a water bath controlled by the electrical heater with a stirrer. The catalyst performance was studied under different reaction conditions, but constant reaction temperature at 65 °C and catalyst particle size >150 μm. The MeOH/oil molar ratio was investigated at 1:35, 1:45, and 1:55. The catalyst loading used were 5, 7, 10 and 15 wt %. The reaction was performed at different times, namely 2, 4, 6, and 8 h.

2.2.4. Methyl ester conversion

The FFA conversion was determined according to the changes in acid value between the WVO before and after the esterification process and calculated from Eq. (3) [21]. The acid value of waste vegetable oil was determined according to the BS EN and ISO 660 (National Standard of the People's Republic of China. GB/T5530-1998), where, AV_0 and AV_1 stand for the acid value of WVO before and after esterification process respectively [22].

$$\text{FFA Conversion } \% = \frac{AV_o - AV_1}{AV_o} x100\% \quad (3)$$

Meanwhile, transesterification conversion was determined by methanol test. WVO conversion of biodiesel was defined according to Eq. (4), where W_o and W_1 stand for the initial WVO weight and unconverted oil weight respectively [8].

$$\text{Transesterification Conversion } \% = \frac{W_o - W_1}{W_o} \quad (4)$$

2.3. Analysis

2.3.1. Spectroscopic analysis

Morphology of olive cake, alkali lignin, bio-char, and prepared catalysts were obtained with an F50 High Vacuum ~ 6e-4 Pa (Eindhoven, Netherlands)-Emission Scanning Electron Microscope (SEM) equipped with an energy dispersive X-ray (EDX) BRUKER QUANTAX EDS system, X Flash Detector 410-M Silicon Drift (SDD), (Berlin, Germany).

The chemical structure and functional groups of olive cake, lignin, bio-char, and the prepared catalysts were examined by Fourier Transform Infrared Spectroscopy (FT-IR), Shimadzue IR pristige-21 system.

X-ray Diffraction (XRD) was used to investigate the crystallinity of olive cake and prepared catalyst using Shimadzue XRD 6000, Cu Kα1 radiation ($\lambda = 1.5418^{o}$A, 30 Kv, 30 mA). Crystallinity index (CrI) was calculated using the Segal method. CrI is determined by the ratio of the maximum intensity of the peak at the 002 lattice diffraction or "crystalline" peak to the intensity of the "amorphous" peak in the same units at 2 $\theta = 18°$ [23].

2.3.2. Olive cake gravimetric analysis

The moisture content of olive cake was determined by placing 1 g of sample in a drying oven (Memmert, T up to 350 °C) at 105 ± 2 °C to constant weight [24].

Ash content of olive cake and alkali lignin was determined by the gravimetric method according to the TAPPI T211 om-07 standard in a muffle furnace (Barnstead thermolyne 6000 furnace) [25].

Lignin content of olive cake was determined as Kalson lignin according to the American Society for Testing and Materials (ASTM: E1721-01) using H_2SO_4 (72%) [26].

2.3.3. Catalyst density

1. The density of SO_3H groups

The number of strong acid sites ($-SO_3H$) in the sulfonated carbon-based catalyst was determined by ion exchange capacity (measuring the amount of H^+ exchanged with Na^+) following the procedure reported by Sani et al. [27].

2. The total acid density of the catalyst

For measuring the total acidity, the contribution of the total acidic group (sulfonic acid, carboxylic acid, and hydroxyl groups), was expressed by the method reported by Lee [28].

3. Results and discussion

3.1. Olive cake characterization

Moisture and ash analysis revealed that Jordanian olive oil cake biomass consisted of moisture (6.95% ± 0.2), and ash contents (2.07%). Similarly, previous studies Ouaini et al. [29] and Brlek et al. [30] showed moisture and ash contents of olive cake biomass as (6.92–7.1%) and (1.7–2%) respectively. The ash content inversely proportional to lignin content, therefore low ash content (2.07%) of olive cake indicated high lignin levels, therefore increasing char and catalyst yields [31,32], while the relatively high moisture content of olive cake increased the lignin yield [33,34]. These results make olive cake an excellent feedstock for lignin-derived catalyst preparation.

The total extractives content (TEC) for the olive cake was relatively high (35%) due to the high content of FFAs, triglycerides, and phenols in the olive cake. Previous studies Hindi et al. [35] and Karimi and Taherzadeh et al. [36] showed that the presence of high extractives into the lignocellulosic biomass is not preferred due to their interference with the hydrolysis reagents used to separate their components and with some component analysis, particularly lignin. This study revealed that the lignin content of olive cake was 52.3% when the extractives were not separated, whereas the lignin was 51.2% when the extractives were extracted before the analysis. This means that there was no more than a 2% difference in the lignin analysis when the extractives were not separated before the lignin analysis. Certainly, this step is time-consuming and will add additional cost to lignin separation process and rarely used for the analysis of lignocellulosic biomass pretreatment and biofuels production.

Lignin content in the olive cake was determined as Kalson lignin. The total yield of kalson lignin obtained from Jordanian olive cake was about 52.3 ± 1.5 wt %. According to literature, the lignin fraction, in olive cake, varies from 20% to 43% [29,34,37,38]. The result obtained from this study was higher compared with previous studies. These differences may be related to the olive chemical composition, the extraction process, or the storage conditions.

The FT-IR spectrum olive cake in the wavelength region from 4000 to 500 cm^{-1} is shown in Fig. 1. The strong band located at 3284.33 cm^{-1} corresponded to stretching of OH group. The band located at 2920.39 cm^{-1} corresponded to the C–H vibrations in methyl and methylene groups. The olefinic (C=C) vibrations cause the emergence of the band at about 1611.03 cm^{-1}, while the = C–O stretching phenols vibrations in aromatic rings causes another band at 1237.76 cm^{-1}. The vibrations at 1422.99 cm^{-1} were

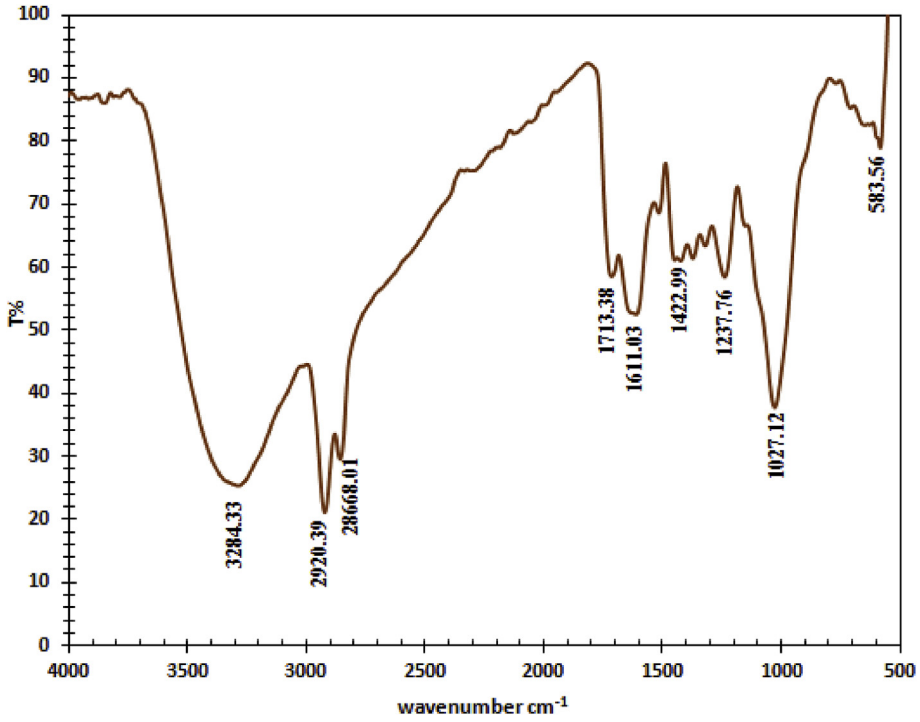

Fig. 1. FT-IR spectrum of olive cake.

assigned to the bands $-CH_3$ and $-CH_2-$. The band at 1237.76 cm^{-1} have been attributed to C–O–H deformation and C–O stretching of phenolics plus an asymmetric C–C–O stretching of esters depending on the attached group. The relatively intense band at 1027.12 cm^{-1} can be assigned to alcohol groups (R–OH) [39].

Fig. 2 illustrates the XRD patterns of olive cake. The diffractograms display a well-defined main peak at around $2\theta = 21.02°$, associated with the diffraction plane (002) of cellulose I. A broad weak diffraction peak in the range of $2\theta = 13°$-$15°$ corresponds to (101) crystallographic planes of cellulose. The small peak at 34.5° assigned to the (040) reflections of cellulose and corresponds to cellobiose unit (two β-glucose molecules linked by a β (1 → 4)) bond.

Crystallinity is strongly influenced by the biomass composition. The raw olive cake presented low relative crystallinity (26.52%) because it has a higher content of hemicellulose and lignin, which are amorphous.

Scanning electron microscope (SEM) was used to investigate the raw olive cake morphology (>2 mm) to compare the structure of cell walls before and after deconstruction by chemical

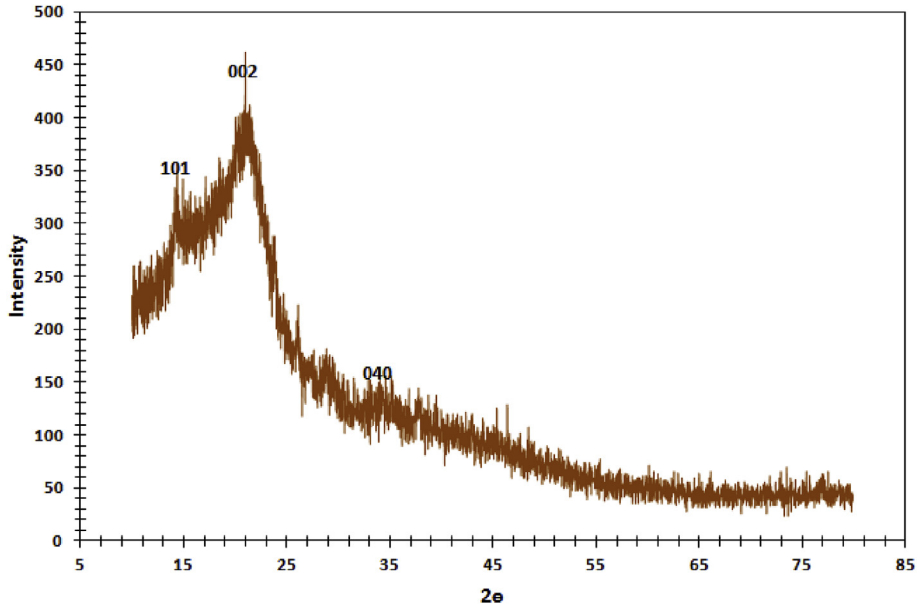

Fig. 2. XRD patterns of olive cake.

pretreatment [40,41]. Fig. 3 showed the internal structure of the olive cake obtained by SEM. The figure indicated that the olive cake has a grainy, rough, and extensive surface area. The surficial elemental composition by EDX analysis revealed the presence of carbon (18.14%), high oxygen (80.94%), (0.92%) potassium, and no sulfur content.

3.2. Lignin analysis

The yield of alkali lignin was 140–170 g per 1 kg of olive cake. The yield was relatively high compared to alkali lignin extracted from steam-exploded olive stones [42].

Delignification efficiency was achieved by determination of kappa no., olive cake after lignin extraction has, as expected, lower kappa no. ($\approx 22.85 \pm 0.16$) and lignin content (3.4%) than the raw olive cake (52.3%). Thus, the results indicated that the delignification efficiency was approximately (93.4%) by alkali extraction.

The isolated alkali lignin had ash content 0.84%. This value was influenced by the process conditions to extract lignin and also related to the high carbohydrates impurities (hemicelluloses and inorganic), about 47.5% reduction in olive cake ash content was observed after the delignification process.

Alkali lignin has an irregular shape, showed partial fragmentation and an increase in surface roughness is clearly indicated and there were no pores visible after the sodium hydroxide pretreatment as shown in Fig. 4, such morphology might be due to alkali treatment conditions of extracting lignin.

Natural lignin, contains phenolic hydroxyl, methoxyl, aliphatic hydroxyl, ketone, and aldehyde functional groups. FTIR of the obtained alkali lignin spectrum was recorded in order to elucidate the structure of lignin and also to investigate the presence of most of the absorption bands: Methoxyl groups, carbonyl groups, and hydroxyl groups.

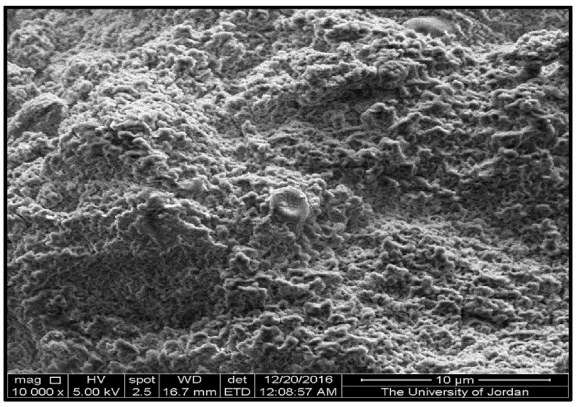

Fig. 4. SEM image of olive cake Alkali lignin.

As shown in Fig. 5, alkali lignin isolated from olive cake showed a wide absorption band around 3347.49 cm^{-1} originated from O–H group stretching of hydroxyl bound to lignin, the intensity of this band variation compared with untreated olive cake proving that the alkali treatment conditions used in the delignification affected the extracted lignin structure. Moreover, this group increases the lightning hydrophilicity and ability to connect to another functional group via H bonds [43,44]. The spectra presented bands between 2919.75 and 2854.40 cm^{-1} that corresponded to the vibration of the C–H bond in methyl and methyl radicals which are common in the lignin structure. The asymmetric deformation of this bond also produced a band at around 1451.28 cm^{-1}. It also indicates the C–H stretching vibration of cellulose/hemicellulose.

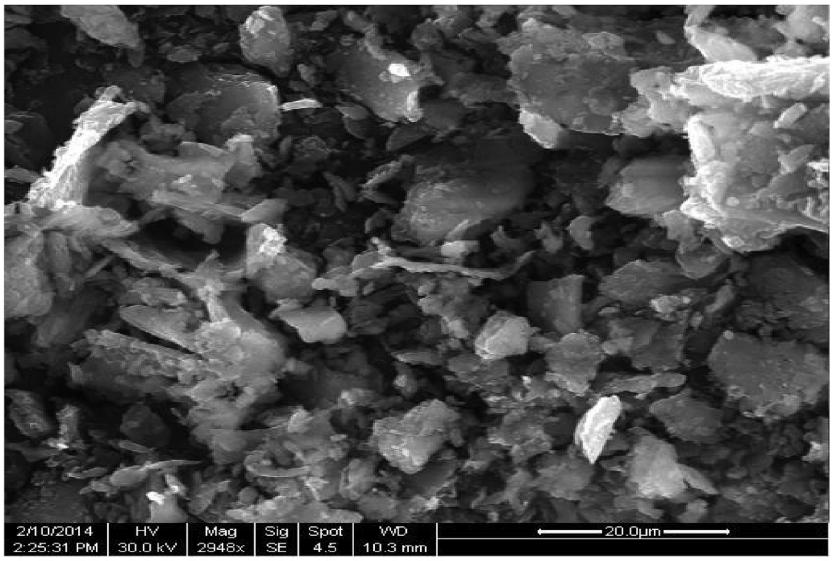

Spectrum: Acquisition 11068

El	AN	Series	unn. C [wt.%]	norm. C [wt.%]	Atom. C [at.%]	Error [%]
C	6	K-series	18.14	18.14	22.91	8.0
O	8	K-series	80.94	80.94	76.73	29.0
K	19	K-series	0.92	0.92	0.36	0.1
		Total:	100.00	100.00	100.00	

Fig. 3. SEM image and EDX of raw olive cake.

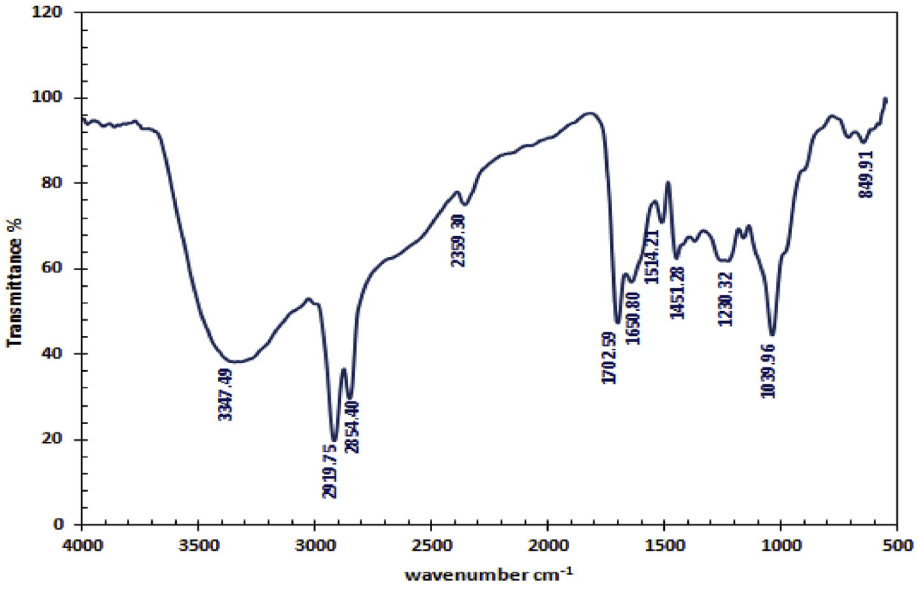

Fig. 5. The FT-IR spectrum of olive cake Alkali lignin (4000-500 cm^{-1}).

Two typical vibrations appeared in the aromatic region, these bands were exhibited around 1514.21 and 1451.28 cm^{-1}. Therefore, phenylpropane units (lignin skeleton) were identified in alkali extracted lignin (1514.21 cm^{-1} render to syringyl lignin characteristic peaks). The vibration at around 1702.59 cm^{-1}, 1650.80 cm^{-1} was associated with the C═O bond stretching in the unconjugated carbonyl group, ester groups indicating the presence of hemicellulose, and conjugated aryl carbonyl group. A high-intensity peak at 1039.89 cm^{-1} attributed to aromatic C—H in-plane deformations.

The signal observed at 1230.32 and at 849.91 cm^{-1} is characteristic of the quaiacyl ring found on the alkali lignin spectrum which indicates the presence of guaiacyl in lignin's chemical structure. Bands occurring from 1650.80 to 1514.21 cm^{-1} are characteristics of aromatic compounds (phenolic hydroxyl groups) and are attributed to aromatic skeleton vibration [45]. The sulfonic acid groups appeared at about 1230.32 cm^{-1}, while, carbonyl group appeared at 1702.59 cm^{-1} and the absorption at 2919.75 cm^{-1} corresponds to the C—H vibration of aliphatic carbon. These results showed that the lignin sample was probably obtained from softwood.

3.3. Char Analysis

Incomplete carbonization of activated alkali lignin at 400 °C in the presence of H_3PO_4 leading to gradual dehydration and dissociation of —C—O—C—, producing amorphous carbon material consisting of small polycyclic aromatic carbon sheets [46] in yields of approximately 70% from alkali lignin.

Surface morphology after lignin pyrolysis was used to determine the structural improvement by forming a porous structure [47]. The char pyrolyzed at 400 °C for 1 h from the phosphoric pretreated alkali lignin is completely different in morphology as compared with the raw alkali lignin, as shown in Fig. 6 the char had a sponge-like structure with minor distribution of pores across the surfaces due to chemical activation by phosphoric acid before the pyrolysis process. The presence of small pores on the lignin bio-char surface enhanced the chances of lignin to incorporate SO_3H group because it promoted dispersion and penetration of the sulfonic group into the lignin.

The FT-IR of lignin bio-char is shown in Fig. 7, most bands showed a shift in the wavelength after carbonization. The exact reason for that is the intensity of the absorbance due to the hydrogen bonded OH stretching decreased by increasing temperature. The decrease may be due to the loss of phenolic or alcoholic groups since the oxygen/carbon ratio decreased. The high-intensity peak in the 3347.49 cm^{-1} regions observed for alkali lignin was transformed into a broader and weaker signal peaked at 3488.05 cm^{-1}, illustrating the decrease in the number of OH-groups present after carbonization.

Lignin bio-char contained relatively a large amount of polycyclic aromatics as it is demonstrated the bands at 1136.69 cm^{-1} due to Ar—OH stretching and at 1443.33, 1577.26 cm^{-1} due to C═C stretching. With these bands intact, the sulfonation developed a distinguished absorption at 1023 cm^{-1}. At 400 °C, aliphatic CH_3 and CH_2 were decreased. These two groups contributed to the most peak intensity at 2914.73 and 2850.48 cm^{-1} of raw lignin [48]. Ar—CO—CH_3 which mainly corresponded to the methoxyl group also decreased after carbonization as a result of the removal of hydrogen.

The partial carbonization has a significant effect on the char surface area. The results showed that the lignin/H_3PO_4 mixture of 1:1 (w/w) solid to liquid ratio, activated at 400 °C for 1 h has a significant effect on lignin surface area. The surface area of lignin was increased from 1.078 m^2/g to 934.5 m^2/g after carbonization; this might be due to an attack on the structure by the strong acid. This result was relatively high compared to the pyrolyzed kraft lignin char with phosphoric acid pretreatment [17].

3.4. Catalyst characterization

The surface structure where the reactants and the products are transported in and out of the catalyst is the key to catalyst activity [49]. The SEM images revealed that the size of the catalysts particles decreased slightly, it was clear that specific surface area and pore volume of $LACS_1$, $LACS_5$, and $LACS_{10}$ sulfonated catalysts decreased due to the penetration of acid groups (SO_3H) on the surface of porous char, the structure became less spongy (when compared with bio-char) as shown in Fig. 8 (a, b, c), respectively. Moreover, a structural destruction and collapse were observed in $LASC_{10}$, this may be due to the long sulfonation time.

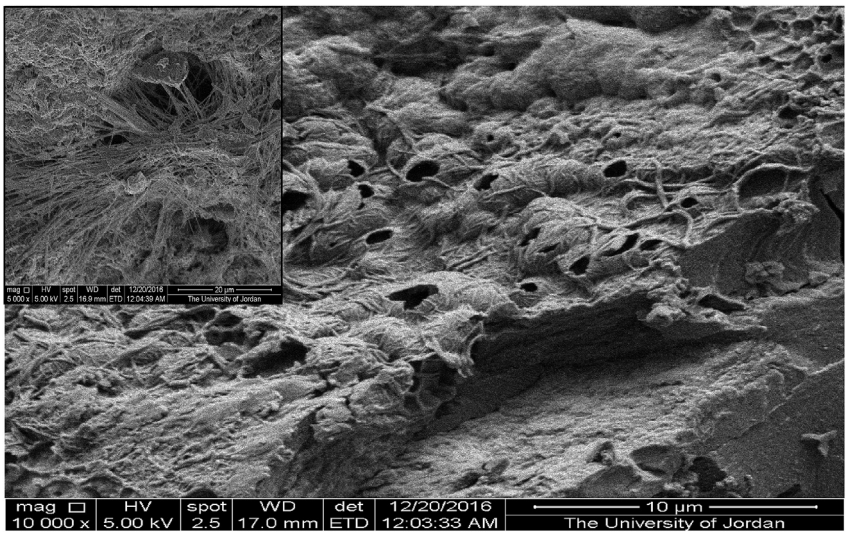

Fig. 6. SEM images of biochar obtained from alkali lignin at different magnification.

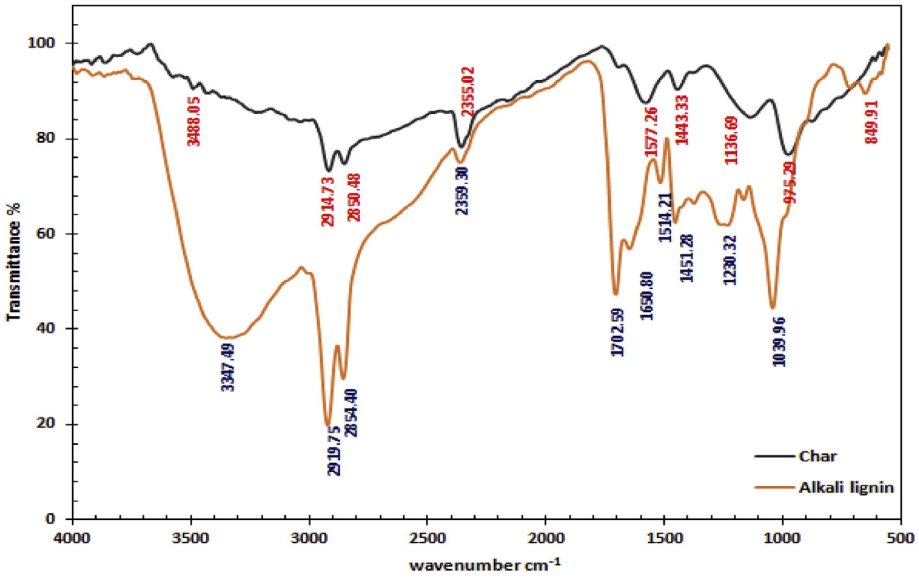

Fig. 7. FT-IR spectra of alkali lignin, biochar (4000-500 cm^{-1}).

The XRD pattern of sulfonated alkali lignin at different sulfonation times exhibited a similarly wide and broad C (002) diffraction peak around ($2\theta = 10°–30°$) assigned to an amorphous cross-linked phenylpropane-based lignin oriented in a random fashion as shown in Fig. 9. The weak and broad C (101) diffraction peak ($2\theta = 35\text{-}50°$) is due to the axis of the graphite structure. This indicated that the samples were comprised of a high content of non-graphitic carbon structure. When sulfonation time increases from 1 h to 5 h, the peak intensities further increased and then decreased to 10 h. The intensities were found to be the lowest for $LACS_{10}$. The decreased in peak intensities were due to attachment of abundant $-SO_3H$ groups to the carbon sheet leading to an increased disorder among graphitic carbon sheets at higher sulfonation time. Lignin was heated at 400 °C under nitrogen condition and the C–O–C bonding of the structure started to break the cleavage of the bonding. Due to this reason, the amorphous structure and the formation of polycyclic carbon sheets became clearer. This may be important in the catalyst's activity during the esterification process. The results were similar to those of amorphous carbon prepared by carbonization and sulfonation as reviewed by Guo and Fang [50].

Crystallinity index calculation by Segal method suggests that the CrI of sulfonated alkali lignin catalysts were lower than the olive cake biomass indicating an increase in amorphous carbon structure after sulfonation of as shown in Table 1. The crystallinity index decreased by increasing the sulfonation time from 1 to 5 h, indicating an increase in the attachment of abundant $-SO_3H$ groups and then increased at 10 h sulfonation time, again indicating decrease the attachment of $-SO_3H$ groups to the carbon sheet [51]. These results are in agreement of FT-IR and SEM results.

Sulfonation reaction which is a process of introducing SO_3H groups into carbon materials with a chemical bond to concentrate sulfonic acid is highly time-dependent. The FT-IR analysis of lignin-based solid acid catalyst confirmed the formation of a sulfonic acid functional group as shown in Fig. 10. The sulfonated bio-char shows peaks at around 1570 cm^{-1} attributable to an aromatic ring. Peaks around 1020 and 1160 cm^{-1} (O=S=O stretching) indicate the

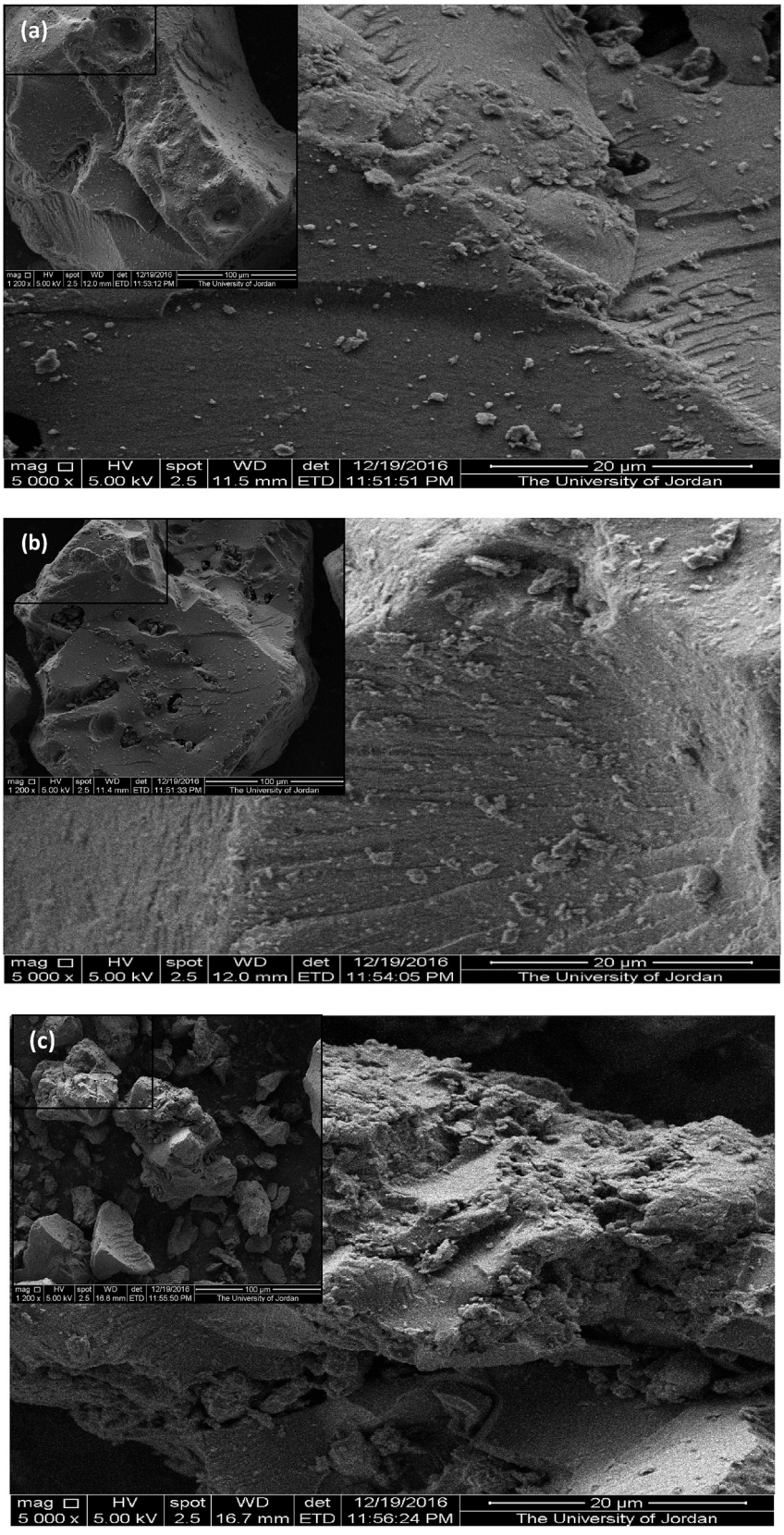

Fig. 8. SEM images of sulfonated catalysts at different sulfonation time (a) $LACS_1$, (b) $LACS_5$ and (c) $LACS_{10}$.

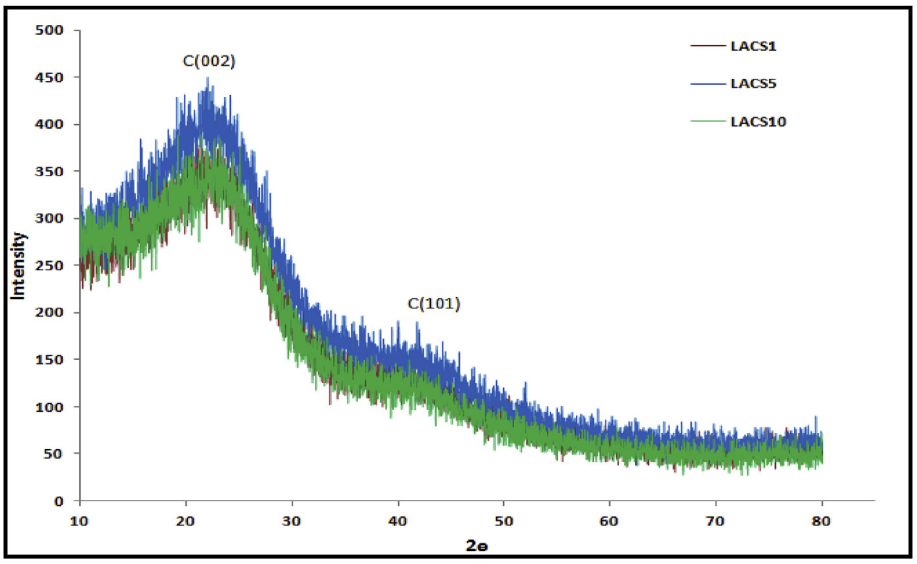

Fig. 9. XRD patterns of sulfonated catalysts ($LACS_1$, $LACS_5$, $LACS_{10}$).

Table 1
Crystallinity index of lignin-based solid catalysts.

Catalyst	CrI%
Olive cake	26.52
$LACS_1$	13.36
$LACS_5$	9.79
$LACS_{10}$	15.69

presence of SO_3H groups. This confirms the incorporation of sulfonic groups onto the carbon matrix after sulfonation [52]. In the presence of concentrated H_2SO_4, aliphatic CH_3/CH_2 groups are oxidized to the carboxylic group (−COOH), which may further increase the total acid densities. The bands around 1690 cm^{-1}, which can be assigned to C═O stretching for (COOH) groups, show that carboxyl acid groups are also present at the surface of the lignin-based solid acid [51].

By comparison of the three types of the catalyst as shown in Fig. 11. The $LACS_5$ possessed the highest SO_3H and total acid densities. Moreover, the observed effect of increasing the sulfonation time to 10 h led to reduced total acid site densities thereby, having low catalytic performance in both esterification and transesterification reactions.

It was concluded that sulfonation reaction needs a certain reaction time for introducing the $-SO_3H$ groups into the partially carbonized alkali lignin. The reaction was completed within 5 h. Nevertheless, by increasing the sulfonation time to 10 h, a structural destruction and collapse were accompanied with SO_3H functionalization. This was confirmed by a decrease in the absorbance of the sulfonic acid functional group [53]. Also, both −COOH and $-SO_3H$ groups were successfully formed on the solid acid after sulfonation as shown in Fig. 11.

After sulfonation, it is obvious as shown in Table 2 that the surface of pores within bio-char was potentially occupied by ($-SO_3H$) groups. Therefore, the surface area decreases with

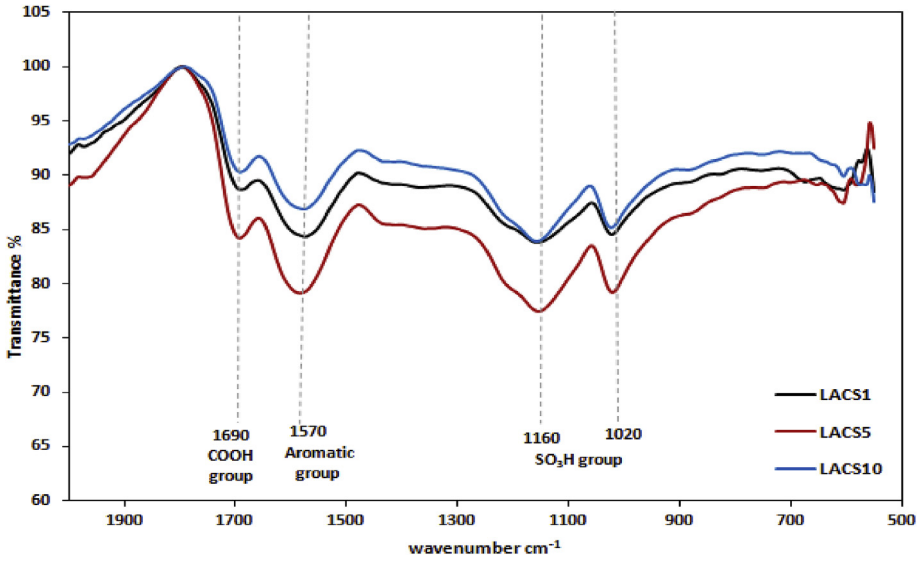

Fig. 10. FT-IR functional groups of sulfonated catalysts ($LACS_1$, $LACS_5$, $LACS_{10}$).

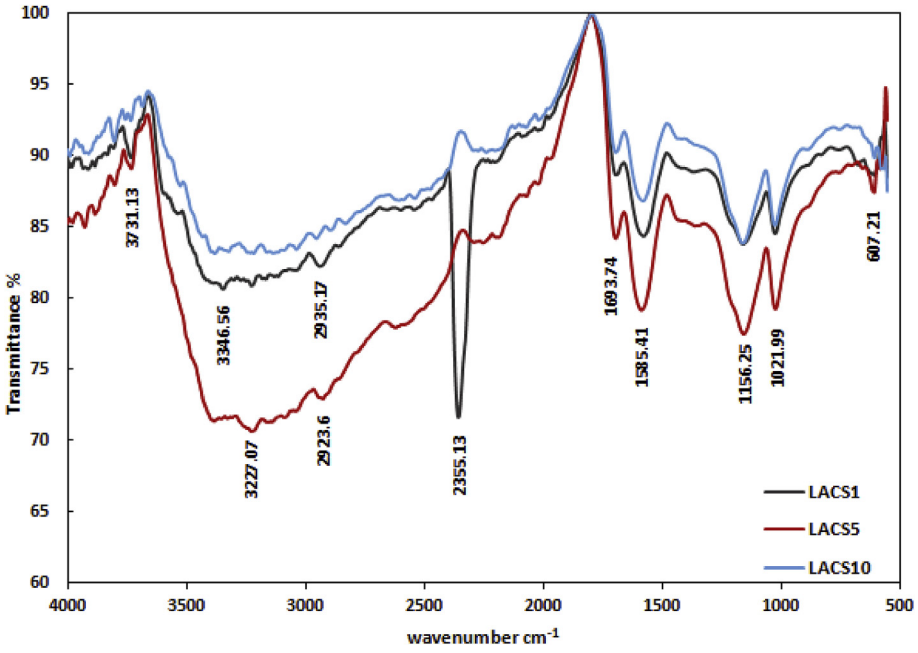

Fig. 11. FT-IR Spectra of sulfonated catalysts ($LACS_1$, LACS5, $LACS_{10}$).

increasing sulfonation time. This probably due to the oxidation reaction between carbon and sulfonic acid molecules. The results indicated that the chemical activation with phosphoric acid increases the BET of lignin while the surface area decreases significantly after sulfonation due to penetration of acid groups on the surface of porous char. This is consistent with the results reported by Pua et al. [17].

These results are also consistent with the EDX spectra for the sulfonated lignin bio-char as shown in Fig. 12 (a, b, c) which revealed that S content increased from 5.58 to 6.42 wt% by increasing the sulfonation time from 1- to 5 h and then decreased to 4.85 at 10 h (assuming that all S atoms in the catalysts were in $-SO_3H$ form). The results are in good agreement with the data from the Pue et al. [17].

On the contrary, Hidayat et al. [54] reported that the BET of coconut shell bio-char after sulfonation in concentrated H_2SO_4 at 150 °C for 24 h was increased from 161.29 to 244.23 m^2/g. Furthermore, homogenization with succinic acid after sulfonation showed a higher surface area, pore size and pore volume than non-homogenized sulfonated catalyst as investigated by Sani et al. [27].

Acid densities of prepared catalysts are consistent with the FT-IR, and EDX results as summarized also in Table 2, a comparison between the $-SO_3H$ density-the total acid density of alkali lignin-derived catalyst and other previous lignin-derived catalyst are shown in Table 3. It is obvious that the catalyst was sulfonated for 5 h showed the highest SO_3H group density (0.69 mmol/g). This value was much lower than that of the commercial ion exchange resin (Amberlyst-15), (4.66 mmol/g) as shown in Table 3. While the total acidity expressed as a sum of all acidic groups such as phenolic OH, carboxylic CO2H, and sulfonic SO3H were found to be similar to that of the well-known ion exchange resin Amberlyst-15.

3.5. Catalyst activity

A series of batch studies were conducted by one step transesterification reaction of non-pretreated waste vegetable oil (3.67 mg KOH/g acid value) with methanol. Conversions from the three types of sulfonated Alkali lignin ($LACS_1$, $LACS_5$, and $LACS_{10}$) were compared.

3.5.1. Effect of reaction time

It was observed as shown in Fig. (13-a, b, c, d, e, and f) that the transesterification and esterification conversion increased with increasing the reaction time from 2 to 6 h. However, the conversion was reduced after 6 h reaction time. The unexpected results might be due to the deactivation of catalyst over time or leaching of the active sites ($-SO_3H$) group.

3.5.2. Effect of amount of catalyst

Fig. 14 (a, b, c) depicts the effect of the catalyst amount on the transesterification conversion. The amount of catalyst ranged from 5, 7.5, 10 to 15 wt %. Other conditions were the oil/methanol molar ratio of 1:35, 45, and 55, the reaction time of 2, 4, 6, 8, and 10 h, while the reaction temperature was kept constant at 65 °C. As observed at 6 h reaction time, the transesterification conversion increased with an increase in the catalyst amount from 5 to 10 wt % of the three types of catalysts, due to the multiplicity of active sites, the conversion was increased from 39.07 to 56.86%, for the catalyst

Table 2
BET surface area and Acid density of the lignin-derived acid catalyst of alkali lignin-derived acid catalyst.

Catalyst	Sulfonation time (h)	BET (m^2/g)	SO_3H density[a] (mmol/g)	Total acid density (mmol/g)
$LACS_1$	1	10.73	0.456 ± 0.01	4.24 ± 0.28
$LACS_5$	5	9.98	0.69 ± 0.02	4.55 ± 0.12
$LACS_{10}$	10	6.42	0.405 ± 0.03	4.13 ± 0.40

[a] Mean of two values ± STD.

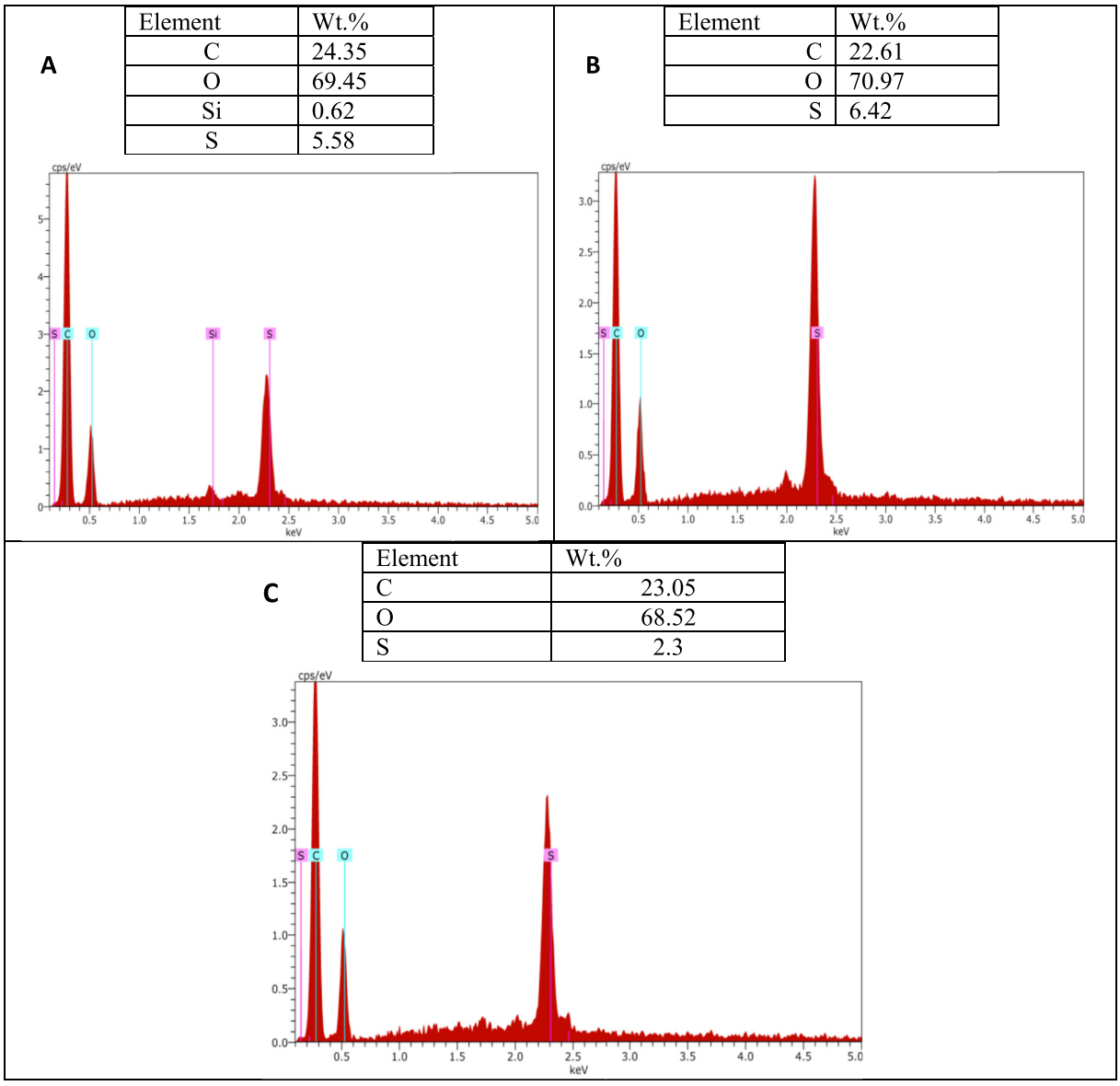

Fig. 12. Energy-dispersive x-ray spectrometry (EDX) spectra of sulfonated Alkali lignin chars (A) $LACS_1$, (B) $LACS_5$ and (C) $LACS_{10}$.

Table 3
Acid density of other lignins –derived acid catalyst.

Lignin type	Lignin source	SO_3H density (mmol/g)	Total density (mmol/g)	Reference
Alkali lignin	Olive cake	0.599	4.25	This study
Kraft lignin (sigma aldrich)	–	1.2	–	[17]
Sulfuric acid lignin	Pine wood	0.37	2.22	[55]
Amberlyst-15	–	4.3	4.7	[55]

($LACS_1$) at 1:35 oil/methanol, 6 h reaction time, which was about a 45.5% increment. However, further addition of the catalyst (15% wt. %) showed no significant increment of transesterification conversion. This was due to the rate of the mass transfer reaching the optimum condition (equilibrium point). Thus, it is obvious that the addition of the catalyst more than 10 wt % do not have much influence on transesterification conversion, moreover, as shown in Fig. 15 (a, b, c) there is no significant esterification conversion increment was reported at much catalyst loading. A catalyst amount of 10 wt% was therefore chosen for the optimum reaction conditions.

3.5.3. *Effect of oil/methanol ratio*

Fig. 16 (a, b, c) show the effect of methanol/oil molar ratio on the esterification and transesterification of WVO, solid acid transesterification of WVO with methanol follows a reversible bath [56]. A higher equilibrium conversion can be achieved only if the rate backward reaction is reduced. By using the methanol in excess, this forces the reaction towards the formation of methyl esters. By using catalyst sulfonated for 1 h ($LACS_1$), the esterification rate remains

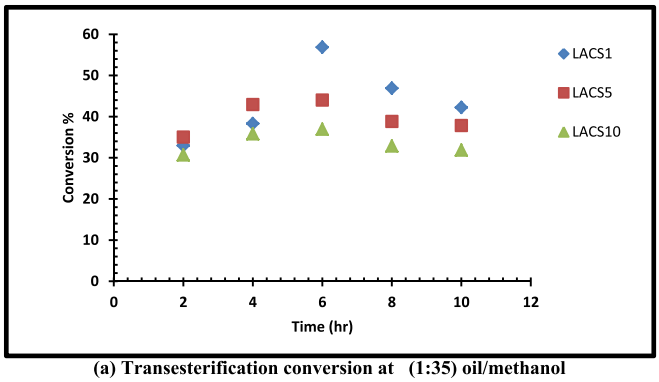

(a) Transesterification conversion at (1:35) oil/methanol

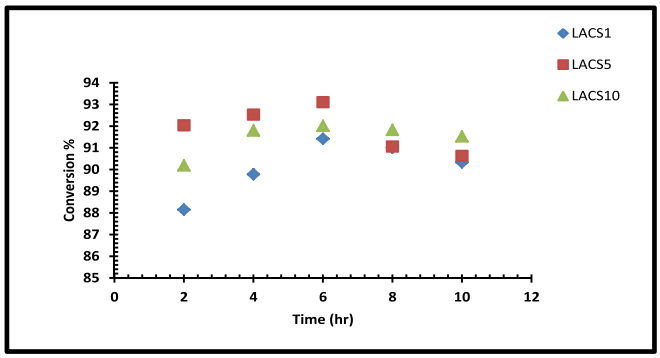

(b) Esterification conversion at (1:35) oil/methanol

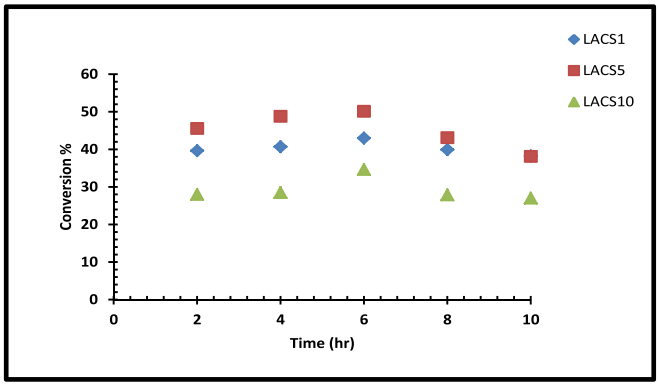

(c) Transesterification conversion at (1:45) oil/methanol

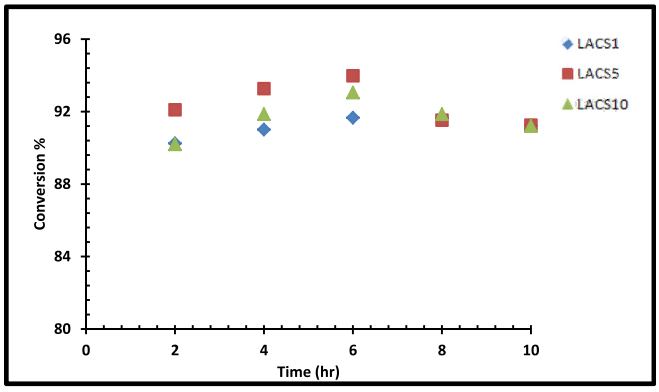

(d) Esterification conversion at (1:45) oil/methanol

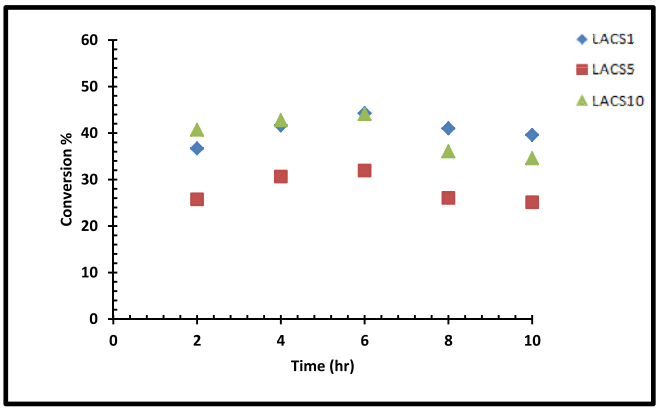

(e) Transesterification conversion at (1:55) oil/methanol

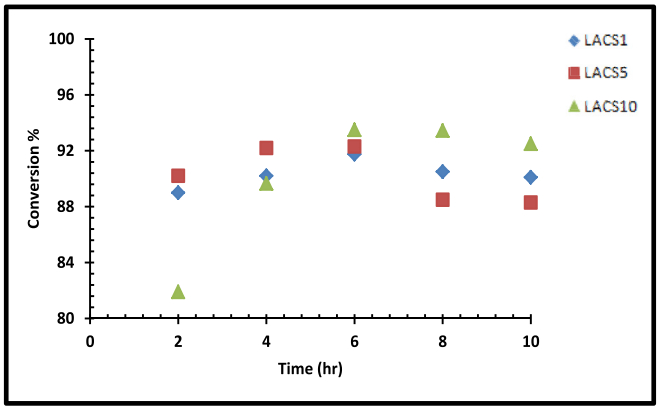

(f) Estrificationconversion at (1:55) oil/methanol

Fig. 13. Effect of reaction parameters on biodiesel production at 10% catalyst loading and different (oil/methanol ratio) (a) Effect of reaction time on biodiesel transesterification conversion at (1:35) oil/methanol, (b) Effect of reaction time on biodiesel esterification conversion at (1:35) oil/methanol, (c) Effect of reaction time on biodiesel transesterification conversion at (1:45) oil/methanol, (d) Effect of reaction time on biodiesel esterification conversion at (1:45) oil/methanol, (e) Effect of reaction time on biodiesel transesterification conversion at (1:55) oil/methanol, and (f) Effect of reaction time on biodiesel esterification conversion at (1:55) oil/methanol.

constant (≈92%) as the oil/methanol ratio increased from 1:35 to 1:55 while the transesterification conversion decreased from 57 to 42% as shown in Fig. 16 (a). This is because the hydrophilic property of the derived lignin acid catalyst was improved by the SO_3H group bonded to the bio-char carbon sheet. However, by increasing the excess methanol, the esterification is accelerated and produces more water. The excessive amount of water caused poisoning of acidic catalysts reduces the acidic hydroxyl OH group because the group becomes hydrated [57]. Another reason might be that the high excess methanol may cause flooding of the active sites which prevent the WVO adsorption on the active sites. Thus, the increased methanol molar ratio inhibited the transesterification conversion. By increasing the sulfonation time from 1 to 5 h as shown in Fig. 16 (b) transesterification conversion increases from 44 to 49% and by increasing the oil/methanol molar ratio from 1:35 to 1:45. However, by increasing the ratio to 1:55, conversion decreases to around 32%. This might be attributed to the more activity of $LACS_5$ than $LACS_1$. This was confirmed by the acid density test, and FTIR analysis. Consequently, the active sites were more and the flooding caused at the high oil/methanol ratio which caused the decreasing in the conversion.

Also by increasing the sulfonation time from 5 to 10 h as shown in Fig. 16 (c), the transesterification conversion increased from around 37 to 44%. Although, by increasing the oil/methanol molar

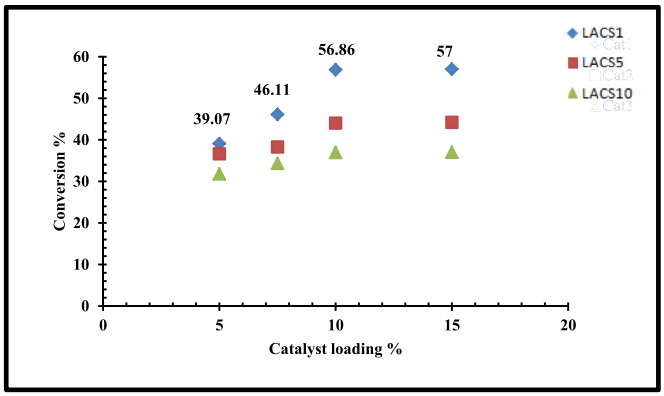

(a) Transesterification conversion of WVO with methanol (1: 35) molar ratio.

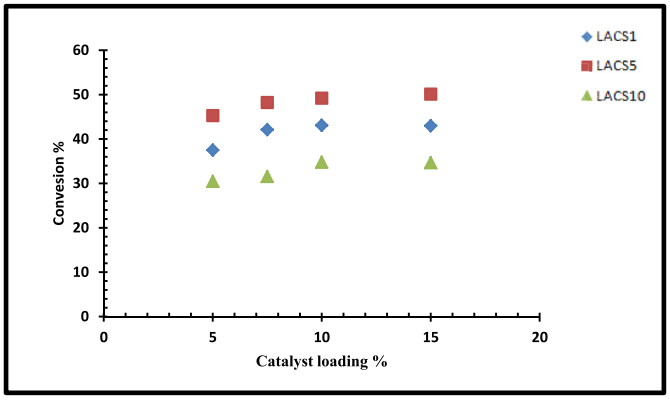

b) Transesterification conversion of WVO with methanol (1: 45) molar ratio.

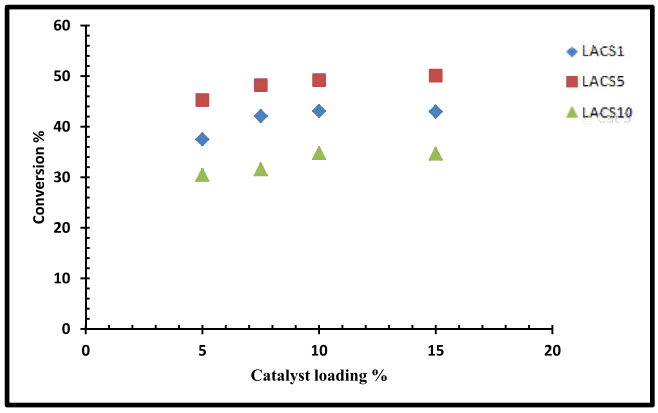

(c) Transesterification conversion of WVO with methanol (1: 55) molar ratio.

Fig. 14. Effect of catalyst loading on biodiesel conversion at 6 h reaction time, a reaction temperature of 65 °C, and different (oil/methanol ratio). (a) Effect of catalyst loading on transesterification conversion of WVO with methanol (1: 35) molar ratio, (b) Effect of catalyst loading on transesterification conversion of WVO with methanol (1: 45) molar ratio, and (c) Effect of catalyst loading on transesterification conversion of WVO with methanol (1: 55) molar ratio.

ratio from 1:35 to 1:55, no decrease in the conversion was observed. This could be due to the decrease in the acid density along with the decrease in the BET surface area.

From the above results, it can be deduced the oil/methanol molar ratio coupled with the acid activity of lignin-derived acid catalyst highly affected the biodiesel conversion.

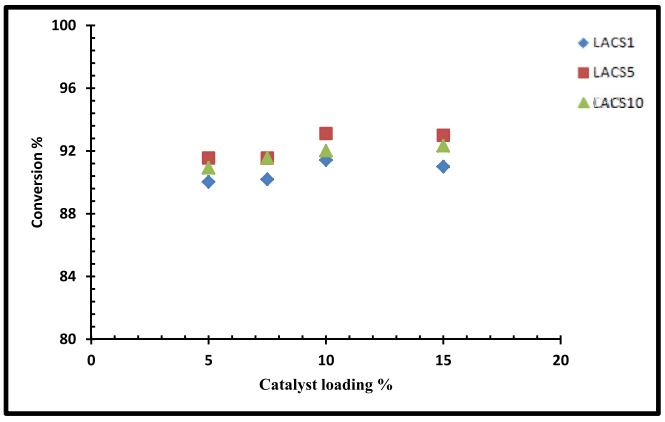

(a) Esterification conversion of WVO with methanol (1: 35) molar ratio.

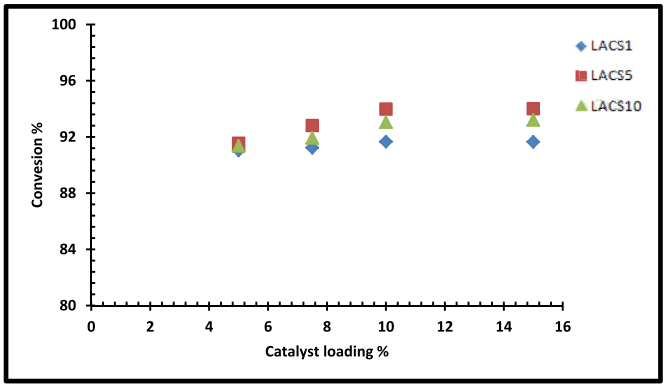

(b) Esterification conversion of WVO with methanol (1: 45) molar ratio.

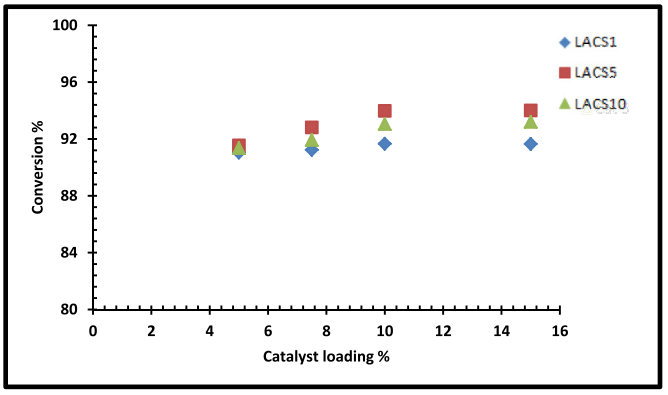

(c) Esterification conversion of WVO with methanol (1: 55) molar ratio.

Fig. 15. Effect of catalyst loading on biodiesel esterification conversion at 6 h reaction time, a reaction temperature of 65 °C, and different (oil/methanol ratio). (a) Effect of catalyst loading on esterification conversion of WVO with methanol (1:35) molar ratio, (b) Effect of catalyst loading on esterification conversion of WVO with methanol (1:45) molar ratio, and (c) Effect of catalyst loading on esterification conversion of WVO with methanol (1:55) molar ratio.

3.5.4. *Effect of sulfonation time*

From the data depicted in Table 4 which summarize the effect of sulfonation time on the catalyst acid density and surface area, it is obvious that the acid density coupled with a specific surface area of lignin-derived acid catalyst highly affects the biodiesel conversion. The reasonable explanation behind the higher activity of $LACS_1$ at low oil/methanol ratio (1:35) against $LACS_5$ and $LACS_{10}$, was that $LACS_1$ possesses the highest surface area. Moreover, the higher

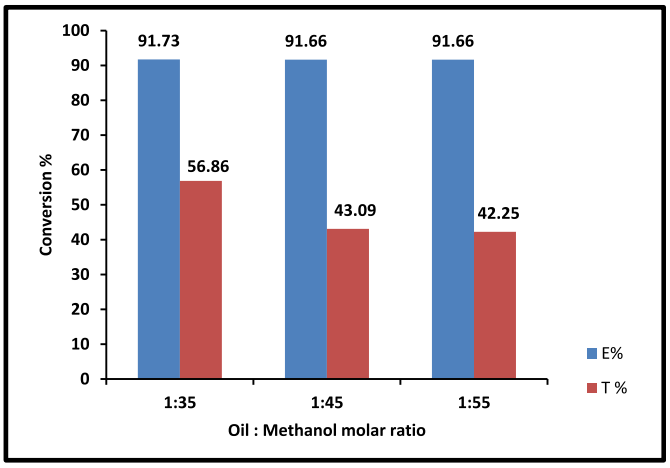

(a) ($LACS_1$)

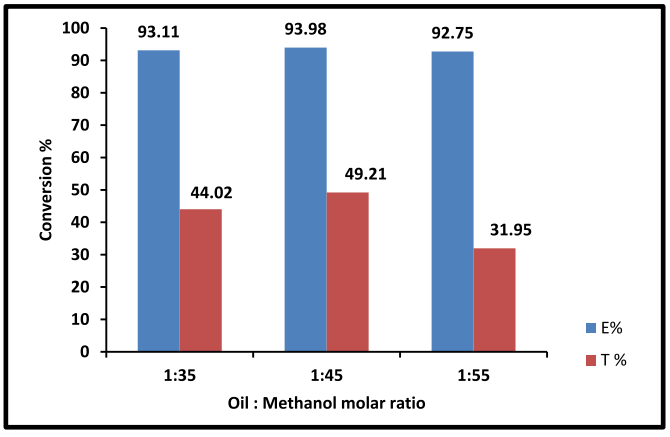

(b) ($LACS_5$)

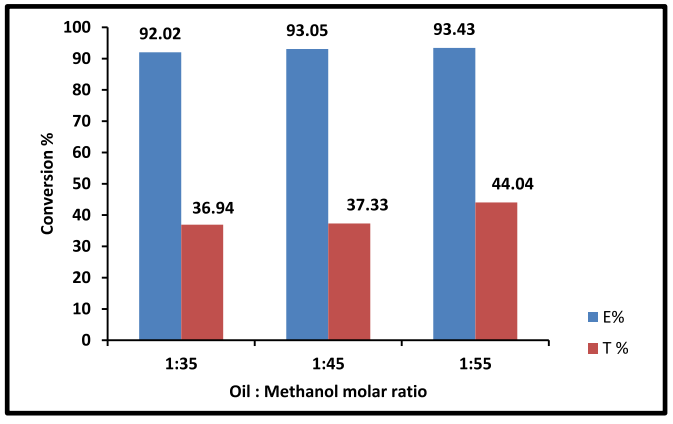

(c) ($LACS_{10}$)

Fig. 16. Effect of oil/methanol ratio on transesterification (T), esterification conversion (E) of WVO at 6 h reaction time, 10% catalyst loading and different sulfonation time.

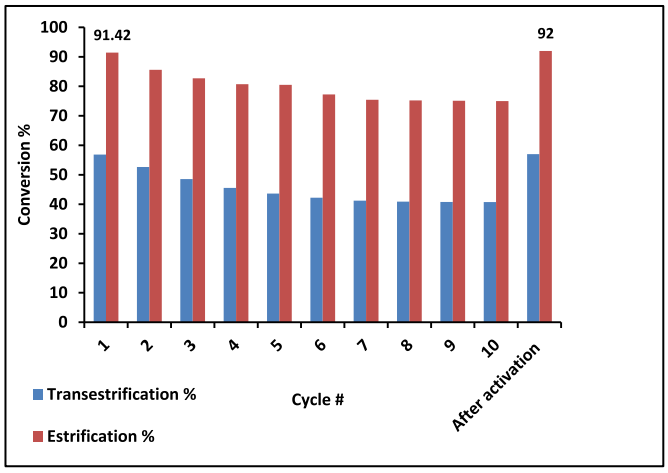

Fig. 17. Reusability test of olive cake lignin-based acid catalyst for esterification, transesterification of WVO under optimized condition.

activity of $LACS_5$ compared to $LACS_{10}$ at 1:45 oil/methanol ratio was due to its higher acid density of strong ($-SO_3H$).

Furthermore, due to the poor mass transfer of solid acid catalysts, a high oil/methanol ratio was needed at lower acid density and surface area to gain the high transesterification conversion which observed in $LACS_{10}$ [57]. This result highlights that the successful incorporation of strong acid density combined with the high surface area is essential for higher transesterification conversion.

3.6. Catalyst reusability

The lignin-based catalyst reusability has been conducted by washing the catalyst ($LACS_1$) with methanol and hexane (commercial grades) at room temperature, followed by drying at 100 °C for 2 h. The recyclability of lignin-based solid acid catalyst was tested for esterification, transesterification of WVO under the optimized condition (6 h reaction time, 1:35 oil/methanol molar ratio, 10 wt% catalyst, and 65 °C reaction temperature). The results show about a 16% decrease in both esterification and transesterification activity even after the catalyst was recycled ten times as shown in Fig. 17. Other lignins-derived catalyst showed a reusability of 3 times [17,49]. It can be concluded that the decrease in the conversion of transesterification was mainly due to the weak interaction between poly-aromatic hydrocarbon structure and SO_3H (leaching of active sites). After activation of the exhausted catalyst with sulfuric acid (98%) for 1 h sulfonation time at 150 °C, the catalyst activity was retained, indicating that the alkali lignin-based solid acid catalyst can be utilized as a stable catalyst.

4. Conclusion

In this work, alkali lignin obtained from the olive cake was incompletely carbonized at 400 °C for 1 h to produce an amorphous polycyclic aromatic carbon structure. Introducing of SO_3H groups

Table 4
Effect of sulfonation time on the catalysts surface area and acid density.

Catalyst	Sulfonation time (h)	Oil/methanol molar ratio	BET (m^2/g)	SO_3H density (mmol/g)	Transesterification conversion %
$LACS_1$	1	1:35	10.73	0.456 ± 0.01	56.86
$LACS_5$	5	1:45	9.98	0.69 ± 0.02	49.21
$LACS_{10}$	10	1:55	6.42	0.405 ± 0.03	44.04

was achieved by sulfonation with concentrated H_2SO_4 at 150 °C for different sulfonation time. The catalysts contain significant amounts of SO_3H, COOH and OH groups. The catalysts were tested for esterification of WVO with methanol. It was found that the catalysts were capable of reducing the acid value of WVO from 3.67 to 0.22 mg KOH/g (which corresponds to about 94% FFA conversion). The optimum variables for the biodiesel production were achieved after a series of reactions within a 6 h reaction time at a 65 °C reaction temperature and 10 wt % of the catalyst. These optimum conditions provided biodiesel conversion about 57% at (1:35) oil/methanol ratio, 49% at (1:45) oil/methanol ratio and 44% of (1:55) oil/methanol ratio for $LACS_1$, $LACS_5$, and $LACS_{10}$ respectively. The difference in catalytic activities was directly related to the SO_3H acid densities and the surface area. The observed 16% catalyst deactivation after 10 times was caused by the leaching of active sites ($-SO_3H$) groups.

References

[1] L.E.D.R. Paula, P.F. Trugilho, A. Napoli, M.L. Bianchi, Characterization of residues from plant biomass for use in energy generation, Cerne 17 (2) (2011) 237–246.

[2] B. Audi, Jordan economic Report, Bank Audi sal-Group Research Department, Bank Audi Plaza, Bab Idriss, Lebanon, 2014.

[3] J.S. Lim, Z.A. Manan, S.R.W. Alwi, H. Hashim, A review on utilisation of biomass from rice industry as a source of renewable energy, Renew. Sustain. Energy Rev. 16 (5) (2012) 3084–3094.

[4] http://www.internationaloliveoil.org/news/view/698-year-2018-news/1082-the-olive-tree-the-most-important-tree-in-jordan.

[5] Ministry of Agriculture, Annual Statistical Report, 2017 (Amman, Jordan).

[6] Z. Al-Hamamre, Potential of utilizing olive cake oil for biodiesel manufacturing, **Energy Sources**, Part A Recovery, Util. Environ. Eff. 37 (23) (2015) 2609–2615.

[7] O.A. Hamed, Y. Foad, E.M. Hamed, N. Al-Hajj, Cellulose powder from olive industry solid waste, BioResources 7 (3) (2012) 4190–4201.

[8] Z. Al-Hamamre, J. Yamin, Parametric study of the alkali catalyzed transesterification of waste frying oil for Biodiesel production, Energy Convers. Manag. 79 (2014) 246–254.

[9] L.T. Thanh, K. Okitsu, L.V. Boi, Y. Maeda, Catalytic technologies for biodiesel fuel production and utilization of glycerol: a review, Catalysts 2 (1) (2012) 191–222.

[10] N. Al-Jammal, Z. Al-Hamamre, M. Alnaief, Manufacturing of zeolite based catalyst from zeolite tuft for biodiesel production from waste sunflower oil, Renew. Energy 93 (2016) 449–459.

[11] E. Ruiz, C. Cara, M. Ballesteros, P. Manzanares, I. Ballesteros, E. Castro, Ethanol production from pretreated olive tree wood and sunflower stalks by an SSF process, in: Twenty-seventh Symposium on Biotechnology for Fuels and Chemicals, Humana Press, 2006, pp. 631–643.

[12] W.J.J. Huijgen, P.J. de Wild, J.H. Reith, Lignin production by organosolv fractionation of lignocellulosic biomass, in: Presented at the International Biomass Valorisation Congress, vol. 13, 2010.

[13] Thomas Ingram, et al., Comparison of different pretreatment methods for lignocellulosic materials. Part I: conversion of rye straw to valuable products, Bioresour. Technol. 102 (8) (2011) 5221–5228.

[14] J. Emrani, A. Shahbazi, A single biobased catalyst for biofuel and biodiesel, J. Biotechnol. Biomater. 2 (1) (2012) 1–7.

[15] A. Toledano Zabaleta, Lignin Extraction, Purification and Depolymerization Study, 2014.

[16] S. Uzuner, R.R.S. Shivappa, D. Cekmecelioglu, Bioconversion of alkali pretreated hazelnut shells to fermentable sugars for generation of high-value products, Waste and Biomass Valorization (2016) 1–10.

[17] F.L. Pua, Z. Fang, S. Zakaria, F. Guo, C.H. Chia, Direct production of biodiesel from high-acid value Jatropha oil with solid acid catalyst derived from lignin, Biotechnol. Biofuels 4 (1) (2011) 56.

[18] A.S. Olawale, O.A. Ajayi, M.S. Olakunle, M.T. Ityokumbul, S.S. Adefila, Preparation of phosphoric acid activated carbons from Canarium Schweinfurthii Nutshell and its role in methylene blue adsorption, J. Chem. Eng. Mater. Sci. 6 (2) (2015) 9–14.

[19] X.J. Jin, Z.M. Yu, Y.U. Wu, Preparation of activated carbon from lignin obtained by straw pulping by KOH and K_2CO_3 Chemical activation, Cellul. Chem. Technol. 46 (1) (2012) 79.

[20] I.M. Lokman, U. Rashid, Y.H. Taufiq-Yap, R. Yunus, Methyl ester production from palm fatty acid distillate using sulfonated glucose-derived acid catalyst, Renew. Energy 81 (2015) 347–354.

[21] T. Liu, Z. Li, W. Li, C. Shi, Y. Wang, Preparation and characterization of biomass carbon-based solid acid catalyst for the esterification of oleic acid with methanol, Bioresour. Technol. 133 (2013) 618–621.

[22] National Standard of the People's Republic of China. GB/T5530-1998,GB/T 5530-1998, Animal and Vegetable Fats and Oils–Determination of Acid Value and of Acidity.

[23] S. Park, J.O. Baker, M.E. Himmel, P.A. Parilla, D.K. Johnson, Cellulose crystallinity index: measurement techniques and their impact on interpreting cellulase performance, Biotechnol. Biofuels 3 (1) (2010) 10.

[24] EN 14774-2:2009, E : Solid Biofuels - Determination of Moisture Content - Oven Dry Method - Part 2: Total Moisture - Simplified Method, 2009.

[25] T. Tappi, T211 om-07 Standard: Ash in Wood, Pulp, Paper, Paperboard Combustion at 550 °C, 2007 (TAPPI test methods).

[26] ASTM: E1721-01, Standard Test Method for Determination of Acid-insoluble Residue in Biomass, ASTM International, West Conshohocken, PA, 2009.

[27] Y.M. Sani, A.O. Raji-Yahya, P.A. Alaba, A.R.A. Aziz, W.M.A.W. Daud, Palm frond and spikelet as environmentally benign alternative solid acid catalysts for biodiesel production, BioResources 10 (2) (2015) 3393–3408.

[28] D. Lee, Preparation of a sulfonated carbonaceous material from lignosulfonate and its usefulness as an esterification catalyst, Molecules 18 (7) (2013) 8168–8180.

[29] R. Ouaini, N. Estephan, H. Chébib, D.N. Rutledge, S. Medawar, R. Daoud, N. Ouaini, Chemical composition of olive cakes resulting from various mills in Lebanon, Agrochimica 54 (6) (2010) 321–330.

[30] T. Brlek, N. Voća, T. Krička, J. Lević, Đ. Vukmirović, R. Čolović, Quality of pelleted olive cake for energy generation, ACS 77 (1) (2012) 31–35.

[31] R. Fahmi, A.V. Bridgwater, L.I. Darvell, J.M. Jones, N. Yates, S. Thain, I.S. Donnison, The effect of alkali metals on combustion and pyrolysis of Lolium and Festuca grasses, switchgrass and willow, Fuel 86 (10–11) (2007) 1560–1569.

[32] N. Sorek, T.H. Yeats, H. Szemenyei, H. Youngs, C.R. Somerville, The implications of lignocellulosic biomass chemical composition for the production of advanced biofuels, Bioscience 64 (3) (2014) 192–201.

[33] B. Nagy, B. Simándi, Effects of particle size distribution, moisture content, and initial oil content on the supercritical fluid extraction of paprika, J. Supercrit. Fluids 46 (3) (2008) 293–298.

[34] C. Valiente, E. Arrigoni, R.M. Esteban, R. Amadò, Chemical composition of olive by-product and modifications through enzymatic treatments, J. Sci. Food Agric. 69 (1) (1995) 27–32.

[35] S.S. Hindi, A.A. Bakhashwain, A. El-Feel, Physico-chemical characterization of some Saudi lignocellulosic natural resources and their suitability for fiber production, J. King Abdulaziz Univ. 21 (2) (2010) 45.

[36] K. Karimi, M.J. Taherzadeh, A critical review of analytical methods in pretreatment of lignocelluloses: composition, imaging, and cystallinity, Bioresour. Technol. 200 (2016) 1008–1018.

[37] F. Nebili, F. Bouachir, Valorisation of the olive cake residue by pyrolysis under water vapour current, JEAS-J. Eng. Appl. Sci. 3 (11) (2008) 848–855.

[38] J.A. Alburquerque, J. Gonzálvez, D. Garcıa, J. Cegarra, Agrochemical characterisation of “alperujo”, a solid by-product of the two-phase centrifugation method for olive oil extraction, Bioresour. Technol. 91 (2) (2004) 195–200.

[39] H.A. Omar, L.A.E.B. Attia, Kinetic and equilibrium studies of cesium-137 adsorption on olive waste from aqueous solutions, Radiochemistry 55 (5) (2013) 497–504.

[40] X.L. Song, X.B. Fu, C.W. Zhang, W.Y. Huang, Y. Zhu, J. Yang, Y.M. Zhang, Preparation of a novel carbon based solid acid catalyst for biodiesel production via a sustainable route, Catal. Lett. 142 (7) (2012) 869–874.

[41] R.K. Gautam, A. Mudhoo, G. Lofrano, M.C. Chattopadhyaya, Biomass-derived biosorbents for metal ions sequestration: adsorbent modification and activation methods and adsorbent regeneration, J. Environ. Chem. Eng. 2 (1) (2014) 239–259.

[42] G. Rodríguez-Gutiérrez, F. Rubio-Senent, A. Lama-Muñoz, A. García, J. Fernández-Bolaños, Properties of lignin, cellulose, and hemicelluloses isolated from olive cake and olive stones: binding of water, oil, bile acids, and glucose, J. Agric. Food Chem. 62 (36) (2014) 8973–8981.

[43] S.P. Leitner, G. Gratzl, C. Paulik, H.K. Weber, Carbon materials from lignin and sodium lignosulfonate via diisocyanate cross-linking and subsequent carbonization, C 1 (1) (2015) 43–57.

[44] I. Bykov, Characterization of Natural and Technical Lignins Using FTIR Spectroscopy, Master thesis, Lulea University of Technology, 2008.

[45] D. Watkins, M. Nuruddin, M. Hosur, A. Tcherbi-Narteh, S. Jeelani, Extraction and characterization of lignin from different biomass resources, J. Mater. Res. Technol. 4 (1) (2015) 26–32.

[46] F.A. Dawodu, O.O. Ayodele, J. Xin, S. Zhang, Application of solid acid catalyst derived from low value biomass for a cheaper biodiesel production, J. Chem. Technol. Biotechnol. 89 (12) (2014) 1898–1909.

[47] S. Ouyang, X. Kuang, Q. Xu, D. Yin, Preparation of a carbon-based solid acid with high acid density via a novel method, J. Mater. Sci. Chem. Eng. 2 (06) (2014) 4.

[48] S. Hu, Y. Wang, H. Han, Utilization of waste freshwater mussel shell as an economic catalyst for biodiesel production, Biomass Bioenergy 35 (8) (2011) 3627–3635.

[49] F. Guo, Z.L. Xiu, Z.X. Liang, Synthesis of biodiesel from acidified soybean soapstock using a lignin-derived carbonaceous catalyst, Appl. Energy 98 (2012) 47–52.

[50] F. Guo, Z. Fang, Biodiesel production with solid catalysts, Biodiesel - Feedstocks Process. Technol. (2011) 339–358.

[51] A.M. Dehkhoda, Developing Biochar-based Catalyst for Biodiesel Production, Doctoral dissertation, University of British Columbia, 2010.

[52] Z. Zhang, M.D. Harrison, D.W. Rackemann, W.O. Doherty, I.M. O'Hara, Organosolv pretreatment of plant biomass for enhanced enzymatic

saccharification, Green Chem. 18 (2) (2016) 360–381.
[5 3] Y. Zhou, S. Niu, J. Li, Activity of the carbon-based heterogeneous acid catalyst derived from bamboo in esterification of oleic acid with ethanol, Energy Convers. Manag. 114 (2016) 188–196.
[54] A. Hidayat, K. Wijaya, A. Nurdiawati, W. Kurniawan, H. Hinode, K. Yoshikawa, A. Budiman, Esterification of palm fatty acid distillate with high amount of free fatty acids using coconut shell char based catalyst, Energy Procedia 75 (2015) 969–974.
[55] F. Liang, Y. Song, C. Huang, J. Zhang, B. Chen, Preparation and performance evaluation of a lignin-based solid acid from acid hydrolysis lignin, Catal. Commun. 40 (2013) 93–97.
[56] M. Wang, W.W. Wu, S.S. Wang, X.Y. Shi, F.A. Wu, J. Wang, Preparation and characterization of a solid acid catalyst from macro Fungi residue for methyl palmitate production, BioResources 10 (3) (2015) 5691–5708.
[57] O. Deutschmann, H. Knözinger, K. Kochloefl, T. Turek, Heterogeneous catalysis and solid catalysts, Ullmann's Encyclopedia of Indust. Chem. (2009).